Available online at www.sciencedirect.com
ScienceDirect
Journal of Power Sources 165 (2007) 185–195
JOURNAL OF POWER SOURCES
www.elsevier.com/locate/jpowsour

A direct methanol fuel cell system with passive fuel delivery based on liquid surface tension

Yuming Yang, Yung C. Liang *

Department of Electrical and Computer Engineering, National University of Singapore, Kent Ridge, Singapore 119260, Singapore

Received 6 October 2006; received in revised form 30 November 2006; accepted 30 November 2006
Available online 19 January 2007

Abstract

The existing direct methanol fuel cell (DMFC) systems are fed with a fixed concentration of fuel, which are either a diluted methanol solution or an active fuel delivery driven by an attached active pump. Both approaches limit the power conversion density or degrade the overall efficiency of the DMFC system significantly. Such disadvantages become more severe in small-scale DMFCs, which require a high conversion efficiency and a small physical space suitable for portable electronics. In this paper, passive fuel delivery based on a surface tension driving mechanism was designed and integrated in a laboratory-made prototype to achieve consumption depending on fuel concentration and power-free fuel delivery. Unidirectional methanol-to-water smooth flow is achieved through the capillaries of a Teflon PTFE (polytetrafluoroethylene) membrane based on the difference in liquid surface tension. The prototype was demonstrated to exhibit a better polarization performance and to last for an extended operating time compared to conventional DMFCs. Its high efficiency and load regulation performance were also demonstrated in contrast to an active DMFC supplied with a constant concentration fuel. The fuel delivery driven by the liquid surface tension effect demonstrated here is believed to be more applicable for future small-scale DMFCs for portable electronics.

Keywords: Direct methanol fuel cell; Passive fuel delivery; Liquid surface tension

1. Introduction

The development of new generation power sources that are more efficient, reliable and environmental friendly has become an important research topic. The overall system simplicity of the energy source is also an important consideration to ensure a low-cost factor and high reliability for commercial applications [1]. In view of such demands and requirements, fuel cell devices have attracted enormous attention in both academic and industrial research for the past 20 years [2,3]. The feasible applications of fuel cells range from stationary power generation, transportation and traction to portable and micro-scale electronics with various fuel cell types distinguished according to the nature of the electrolyte they use [4,5]. Being the youngest member of this family, the direct methanol fuel cell (DMFC) is fueled by an aqueous mixture of methanol and water. Fig. 1 gives the general schematic of the DMFC. It comprises the liquid and gas flow field, diffusion and catalyst layers to both anode and cathode sides. A polymer electrolyte membrane (PEM, normally Nafion®) is sandwiched in between the anode and cathode electrodes to be the proton-conducting medium. Methanol is oxidized at the surface of the anode, which is a platinum/ruthenium (Pt/Ru) coated catalytic electrode, to produce carbon dioxide (CO_2), protons and electrons:

$$CH_3OH + H_2O \rightarrow CO_2 + 6H^+ + 6e^- \quad (1)$$

At the cathode, the electrons from external circuit combine with protons transported through the PEM and oxygen to form water:

$$1.5O_2 + 6H^+ + 6e^- \rightarrow 3H_2O \quad (2)$$

The overall electrochemical power generating reaction inside DMFC is described as:

$$CH_3OH + 1.5O_2 \rightarrow CO_2 + 2H_2O \quad (3)$$

As liquid phase methanol is adopted, the energy density of a DMFC system is higher compared to conventional PEM fuel cells fed by gas-phase hydrogen. Meanwhile, the fuel storage

* Corresponding author. Tel.: +65 68742750; fax: +65 67791103.
E-mail address: chii@nus.edu.sg (Y.C. Liang).

0378-7753/$ – see front matter © 2006 Elsevier B.V. All rights reserved.
doi:10.1016/j.jpowsour.2006.11.059

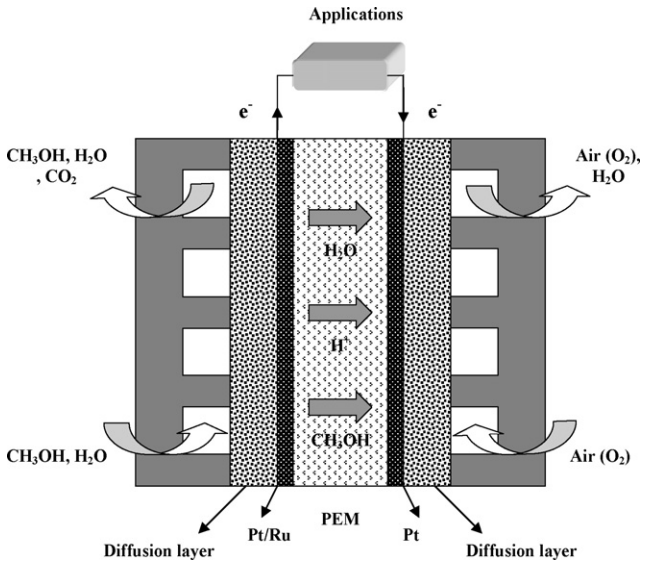

Fig. 1. General schematic of the direct methanol fuel cell (DMFC).

and distribution are much easier for a DMFC without the need of additional components or for pressurized hydrogen. The direct methanol conversion in DMFC under ambient temperature also provides the advantage of omitting any internal fuel reforming steps. Meanwhile, the refreshing of a DMFC by a quick refill of methanol solution without a time-consuming recharging process is advantageous compared with lithium-ion or similar energy storage batteries. All these advantages make DMFC compact, powerful and hence attractive for the small-scale applications.

Despite having promising potential and remarkable breakthroughs recently, there are still a number of issues needed to be addressed before the DMFC can become a commercially viable solution. Among them, the low kinetics of methanol oxidation on the anode catalyst is one major problem limiting the power density of a DMFC [2,6]. Currently, a platinum–ruthenium (Pt–Ru) alloy with an atomic ratio of 1:1 is thought to be the most efficient methanol oxidation catalyst and is commonly used in DMFCs [7,8]. A degradation on DMFC power density comes from the fuel loss at the cathode side, usually called methanol crossover. This phenomenon happens due to the water-filled channels within PEM–Nafion®, which offer a path for methanol permeation through the membrane by means of diffusion and electro-osmotic drag [9]. The crossover of methanol leads to a mixed potential at the cathode due to the direct methanol oxidation on the cathode platinum catalyst. This results in a severe reduction of electrode potential and therefore the overall cell voltage. To overcome such a disadvantage, much work has been carried out on polymer membrane modification and development [10–12]. Nevertheless, the DMFC so far can only function efficiently with a diluted methanol solution to suppress this fuel loss process.

Besides the material research work for cell performance improvement, the concern about fuel storage and delivery in a DMFC system emerges as critical issues for small-scale applications. Generally, these DMFCs have an "active" fuel delivery sub-system to maintain their performance [13]. However, the pumps, sensors and manifolds contained in these DMFCs significantly increase the system complexity and occupy a comparatively big space. Meanwhile, these active components also consume extra power and degrade system efficiency considerably. To compete with state-of-the-art lithium-ion batteries, a fuel-efficient DMFC with compact construction and extended operating time is desirable. Therefore, the approach of zero-power fuel delivery has attracted interest recently in research work on integrating a DMFC into small-scale electronics. However, the most common designs to achieve such a "passive" fuel delivery effect uses a diluted fuel reservoir, which is directly attached to an anode diffusion layer [14–17]. The fuel is delivered to the membrane electrode assembly (MEA) primarily by a natural diffusion process from a reservoir without any power consumption. In such a structure, only diluted fuel is stored in the DMFC to avoid severe methanol crossover. For the same cell volume, such diluted methanol storage reduces the energy density and so shortens operating time remarkably. In recent work, a spring-driven fuel supply mechanism was introduced in the DMFC system design to save on internal power consumption [18]. To improve on the low power density such a mechanism involved diluted fuel formation by driving pure methanol with its spring-based displacement [19]. Although the fuel delivery in such type DMFCs is carried out without power consumption, its spring-driven mechanism still occupies a large space for the mechanical displacement. At the same time, the implanted concentration feedback control system, such as CMOS circuit and valves, still takes additional space.

In this paper, a passive fuel delivery process based on natural liquid physics—surface tension is proposed. The fuel supply subsystem according to this process is designed and demonstrated on a laboratory-made DMFC prototype, which gives the benefit of pure methanol storage and power free fuel dilution. In this prototype, pure methanol is stored in a separate reservoir chamber from the water chamber by a piece of microfibrous structure membrane—a Teflon PTFE (polytetrafluoroethylene) membrane. Due to the difference in surface tension properties, water can be separated from methanol by a Teflon PTFE membrane without leaking into the methanol chamber. However, the forward methanol flow across the separating Teflon PTFE membrane to water chamber can be fulfilled readily via the interconnected capillaries inside the membrane. Accordingly, unidirectional pure methanol delivery and passive fuel mixing can be achieved in this prototype. With this concise auxiliary component, the DMFC is able to operate with zero internal power consumption to improve its efficiency. Moreover, the overall volume of DMFC system can also be reduced significantly, hence facilitating its application in small-scale electronics.

2. Principle and design of passive DMFC prototype

2.1. Theory of the surface tension driving effect

To avoid external energy input, utilizing natural liquid physics is the most preferred approach to drive the liquid flow especially on the micro scale. Surface tension, is known to be a phenomenon arising from the cohesive forces between liquid

molecules, and is such that the pressure scales down quadratically with decreasing linear dimensions [20]. Therefore, it becomes a most advantageous driving mechanism for microfluidic movement.

Inside a bulk liquid body, the cohesive force between liquid molecules is the same in all directions. However, the molecules on the surface feel an unequal force of attraction. The magnitude of the force that controls the liquid surface shape is called the surface tension (σ) [21]. Surface tension is a characteristic property of liquid and is proportional to the strength of the bonds between the liquid molecules. It is defined as the force per unit length (usually dynes cm^{-1}) in the plane of the surface. Depending on the adhesive force between a liquid and solid surface, a liquid shows a different wet characteristic when it rests on a solid surface. Generally, the critical surface tension (σ_C) is used as the primary criteria to identify the hydrophobic or hydrophilic property between a liquid and solid [22,23]. In fact, a liquid will bead up and roll off of a solid material when its critical surface tension is higher than that of the solid material. On the contrary, it will wet the surface easily if material's critical surface tension is greater than that of liquid. Usually, the contact angle (θ) is used as a measurement of the status of hydrophilicity ($0^\circ < \theta < 90^\circ$) or hydrophobicity ($90^\circ < \theta < 180^\circ$).

For the DMFC, the liquids are methanol and water in the fuel. As an organic liquid, methanol exhibits a quite different surface tension from water. At 20 °C, the critical surface tension of deionized (DI) water is 72.8 dynes cm^{-1}, while that of methanol is only 23.7 dynes cm^{-1} [24]. According to above theory, these two liquids will show totally different wet characteristics on a solid material with a critical surface tension between them. Teflon PTFE as a hydrophobic material that is widely used in waterproofing applications. Whereas, it is also a common organic liquid filter, which can be wetted spontaneously by a liquid with σ_C lower than 27 dynes cm^{-1} [25]. Therefore, methanol is expected to wet Teflon PTFE readily while water will bead up due to its hydrophobic properties. The phenomenon is illustrated in Fig. 2(a) with two liquids on a piece of Teflon PTFE tape.

Being a hydrophilic liquid to Teflon PTFE tape, methanol on the Teflon PTFE tape will spread on its surface and diffuse into the tape easily, as can be seen in Fig. 2(a). The liquid diffusion is on the microfibrous structure inside the Teflon PTFE tape, which consists of many interconnected capillaries with diameters ranging from several to tens of microns. On this scale, surface tension becomes a dominant factor over any other forces in the capillary. Therefore, the different transportation of these two liquids in a Teflon PTFE capillary are expected according to their different critical surface tensions. The motions are depicted in Fig. 2(b). The water volume is prevented from filling the Teflon PTFE capillary while methanol is absorbed spontaneously. Such liquid

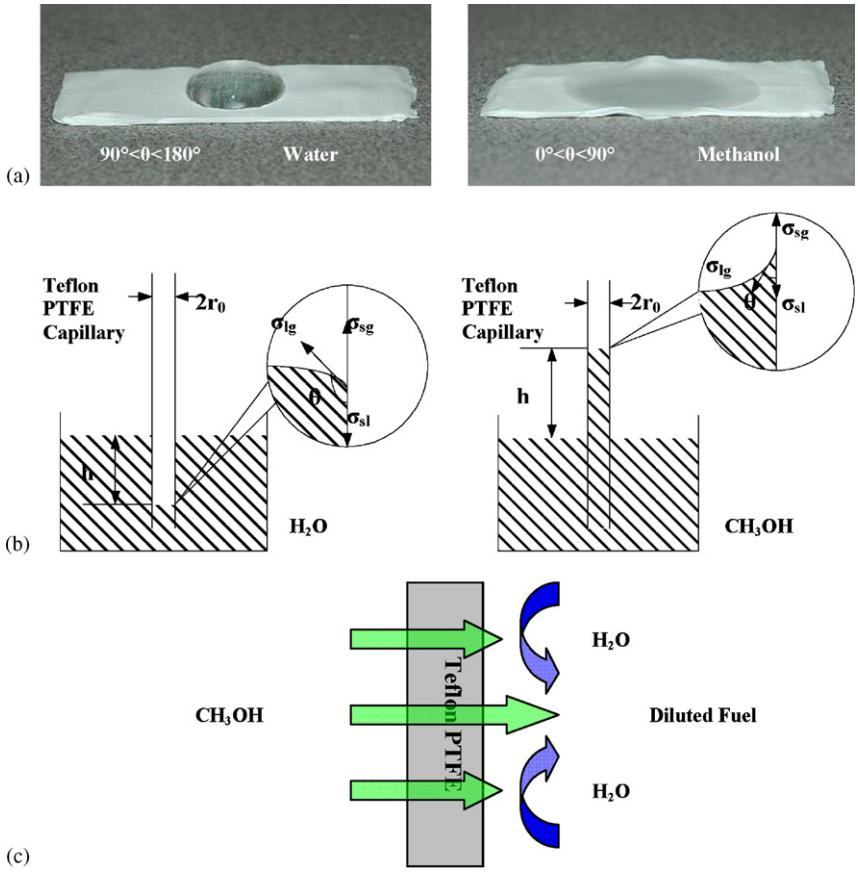

Fig. 2. Different wetting characteristics of water and methanol on Teflon PTFE tape and the explanation of the proposed passive methanol delivery effect. (a) Water and methanol droplets on Teflon PTFE tape, (b) water and methanol motion inside Teflon PTFE capillary and (c) schematic explanation of passive methanol delivery effect.

motion is driven by the pressure difference across the gas–liquid interface. It can be deduced from the balance of surface tensions at the interface of liquid, solid capillary wall and ambient gas [26,27]:

$$\sigma_{sg} - \sigma_{sl} = \sigma_{lg} \cos\theta \tag{4}$$

where σ_{sl}, σ_{lg} and σ_{sg} are surface tensions at solid–liquid, liquid–gas, and solid–gas interface, respectively. θ is the contact angle between solid and liquid interface.

For methanol, the contact angle on a Teflon PTFE capillary wall is less than 90° due to its hydrophilic property and hence the cosine value is positive. From Eq. (4), it can be revealed that solid–liquid interface has a lower surface energy than that of solid–gas interface in capillary. Consequently, the methanol column will move in the direction from liquid to gas across the interface to minimize its surface energy. As the inertia is negligible in the capillary, the energy balance in the liquid column can be described between surface tension and pressure difference across this gas–liquid interface [28]:

$$2\pi r_0 h(\sigma_{sg} - \sigma_{sl}) = \Delta p \pi r_0^2 h \tag{5}$$

in which, r_0 represents the capillary radius.

By combing Eqs. (4) and (5), the pressure difference across the liquid–gas interface Δp can be derived as:

$$\Delta p = \frac{2\sigma_{lg} \cos\theta}{r_0} \tag{6}$$

Obviously, the direction of liquid motion in the capillary can be determined by liquid's contact angle on the sidewall around it. As water shows a hydrophobic property on Teflon PTFE material, its column will then move in the opposite direction to be rejected from the capillary compared to the elevation of methanol column, as shown in Fig. 2(b).

2.2. Objectives and design of a passive DMFC prototype

The completely different liquid motion of methanol and water in one single capillary has been explained. The phenomenon reveals that a unidirectional liquid flow from methanol to water is possible within a capillary. As the motion is only governed by natural liquid physics—surface tension, it can be a spontaneous process to be adopted for passive methanol delivery and fuel mixing without any additional power consumption. The basic working principle to achieve this effect is schematically described in Fig. 2(c). Methanol and water are separated with the Teflon PTFE membrane. Due to its hydrophilic property to Teflon PTFE material, methanol will be absorbed into interconnected capillaries inside the membrane and transported to the other side under surface tension driving force as explained earlier. However, water on the other side is confined from moving into Teflon PTFE membrane due to its hydrophobic characteristic. Therefore, a continuous and unidirectional methanol flow will dominate in the Teflon PTFE capillaries inside this separating membrane. As a result, the diluted methanol solution for DMFC electrochemical reaction is able to be obtained on the water side by mixing with the incoming methanol flow. This mixing process relies on diffusion since methanol can be readily dissolved in water and there is no longer any interface between water and methanol after they get contacted.

Upon applying this concept to a DMFC prototype, instead of loading with diluted methanol solution, these two separated reservoirs are able to carry pure methanol and DI water, respectively. Since the energy content of a DMFC directly depends on the methanol volume fraction, pure methanol storage exhibits the advantage of improving DMFC power density significantly with the same fuel reservoir volume compared to a diluted fuel carrying DMFC. The mixing process occurs along with the capillary delivery effect and diffusion of methanol into water during the entire operation process passively. In the start-up stage of DMFC operation, the reaction kinetics is not drastic enough to consume the methanol contained in conventional DMFCs with fixed concentration fuel effectively. The excessive methanol, therefore, results in the methanol crossover problem and hence the energy loss as well as performance degradation. By reducing the contact area between the Teflon PTFE membrane to water and methanol reservoirs, the unnecessary fast methanol delivery is able to be prevented in this passive prototype. Consequently, the high methanol concentration on water side and accordingly the severe energy loss due to methanol crossover can be avoided at this early operation stage. Once the DMFC operation has started, the fuel consumption will depend on the external load variation. The demand on methanol varies according to the power drain. In a fixed concentration DMFCs, the lack or excess of methanol supply in this situation both degrade the DMFC performance remarkably. Therefore, the adaptive fuel concentration control during its operation is a more attractive improvement in the DMFC. With the proposed passive fuel delivery component, it's the driving mechanism is concentration sensitive. Under a high power drain operation, the methanol content in water chamber decreases due to its drastic consumption. The wettability of liquid in this chamber keeps it relatively hydrophobic. Accordingly, hydrophilic methanol flow dominates in this stage and compensates for the methanol loss by its unidirectional pure methanol flow. When the power drain is reduced, the excessive methanol content in water side will enhance the hydrophilic state of the liquid here. Consequently, a competitive diluted methanol flow is able to come into the capillary of Teflon PTFE membrane from the water chamber to oppose the pure methanol flow from the other side. As a result, a continuous pure methanol supply can be suppressed and the increase in fuel concentration for the reaction can be prevented effectively. With this effect, the self-regulating methanol supply process continuously functions during load variation based on surface tension driving the competitive capillary flow in the membrane. Compared to the constant fuel concentration fueled DMFCs, the adaptive fuel concentration control in the passive prototype has the advantage of both suppressing methanol crossover as well as a low fuel problem and hence improving the efficiency during load variation. Also, the simplicity of this passive fuel supply and mixing makes it more suitable for small-scale DMFC applications.

According to the concept introduced, a fuel supply subsystem was designed and integrated in a laboratory-made DMFC prototype. The detailed structure of this prototype is shown in

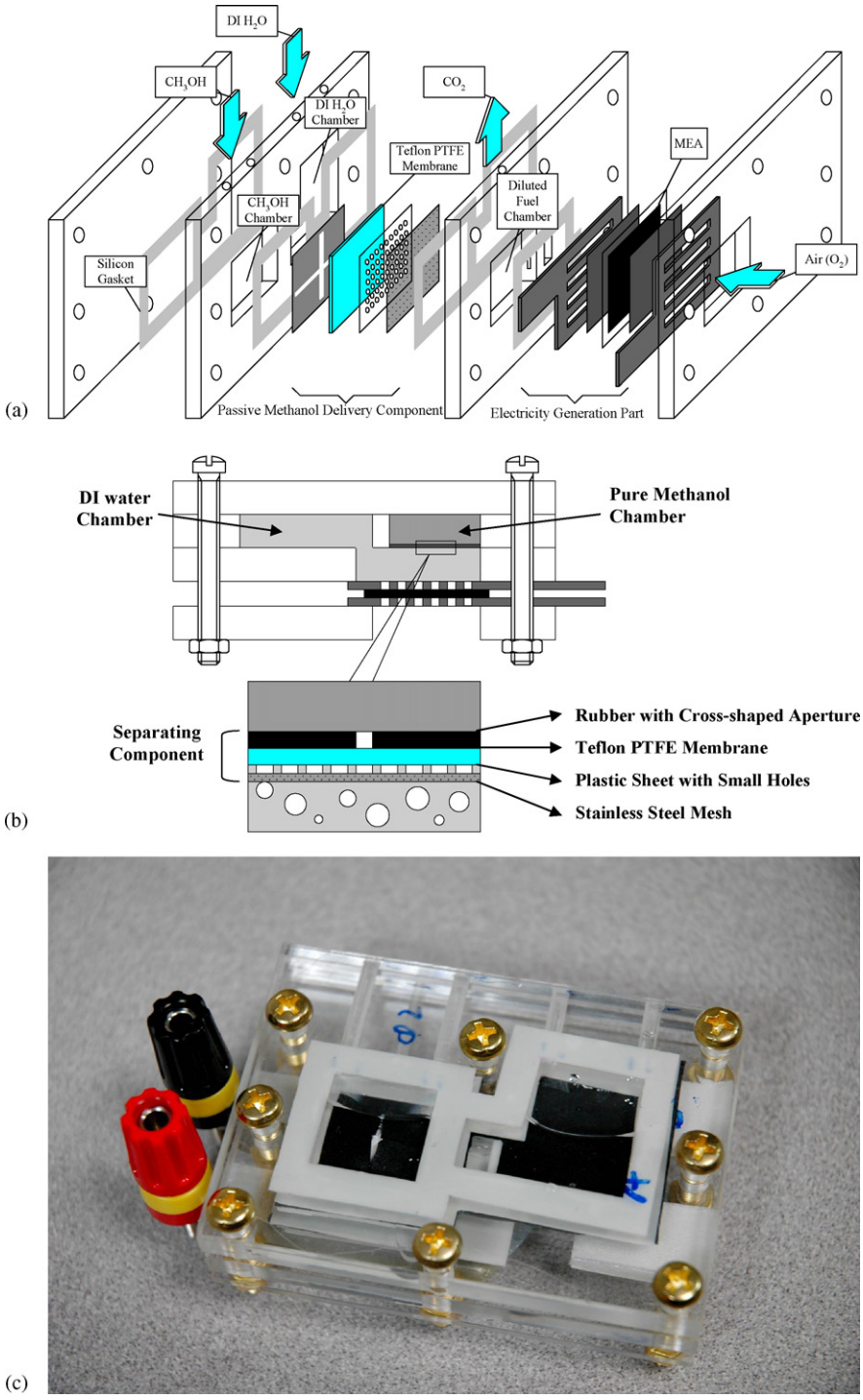

Fig. 3. (a) Schematic of the demonstration prototype, (b) passive methanol delivery process in assembled prototype and (c) assembled demonstration DMFC prototype.

Fig. 3(a). In this prototype, DI water and pure methanol are stored in two different chambers and separated by an eight layers Teflon PTFE membrane (Aldrich) of 1 mm thickness. The chamber volumes are 2 ml for pure methanol and 5 ml for DI water. For the pure methanol chamber, a pair of rubber pins is adopted during the experiments to seal the filling holes to reduce volatilization loss of pure methanol due to its volatile nature. The pure methanol is able to flow into the DI water chamber through the separating Teflon PTFE membrane to form a diluted fuel. With the water chamber connecting directly to the anode side of MEA, the diluted fuel formed there will be used for the electricity generating reaction. Since the critical surface tension of methanol is very low, its outstanding wettability on the Teflon PTFE membrane may cause a sudden increase in methanol concentration on the water side when methanol is filled. Too much methanol in this chamber will exceed the fuel concentration requirement for electrochemical reaction and result in severe methanol crossover. Therefore, some auxiliary components were

designed and adopted to prevent such a phenomenon. On the side of the Teflon PTFE membrane toward pure methanol chamber, a piece of rubber with cross-shaped aperture was attached, while a plastic sheet with an array of small holes was attached on the other side. The 25% open ratio of the plastic sheet was achieved by 40 through-holes with diameter of 2 mm. The reduced open area of these two methanol non-wettable materials decreased the contact area of the membrane to methanol and water on both sides remarkably. Accordingly, the diffusion rate of methanol through the membrane to water will be suppressed effectively. In addition, a piece of 0.5 mm thick stainless steel mesh was attached just behind the plastic sheet on water side of Teflon PTFE membrane. The small square meshes on it help to ensure an even diffusion of methanol into water chamber. On cathode side of MEA, it opened to the ambient through the diffusion layer to provide an oxygen supply from air via natural convection. The DMFC prototype is expected to operate with passive reactants (methanol and oxygen) supply efficiently. The schematic on passive fuel mixing and supply process in assembled prototype is given in Fig. 3(b).

3. Experimental setup

The assembled DMFC prototype is shown in Fig. 3(c), respectively. After assembly, the prototype proceeded to undergo polarization output, operating time, efficiency, and load regulation measurements in the following experiments. The results were compared with those from a constant diluted fuel passive DMFC and external active pump supplied DMFC hardware. The same power generating components including the MEA and diffusion layers were applied on three different types of DMFCs to ensure performance comparison. This MEA had an active area of 2.24 cm × 2.24 cm. Nafion® 117 membrane was used as the protonic membrane. The anode catalyst loading on the membrane was 2 mg cm^{-2} using platinum–ruthenium (Pt–Ru) black with an atomic ratio of 1:1 for methanol oxidation. On the cathode side, only platinum (Pt) black was used as the catalyst for oxygen reduction with the same loading of 2 mg cm^{-2}. Before the MEA was assembled into the experimental DMFC hardware, a pre-treatment was carried out to improve its performance. The MEA was first rinsed in DI water at 50 °C for 2 h. After that, it was soaked in diluted methanol solution of concentration 3 M overnight at room temperature (25 °C). The pre-treatment of the MEA helped to avoid the dry state and improve the activity of the membrane as well as the catalyst sites. Accordingly, the DMFC was able to achieve a relatively quick start-up [29]. When assembling the MEA into the cell, a pair of carbon papers – E-TEK B-1 Type A for the anode and E-TEK ELAT® LT1400-W for cathode – were attached as diffusion layers. The current collectors were made of stainless steel with an open area for reactant transport on both sides. In the DMFC performance measurements, the setting of different ambient temperatures for operation was achieved by a temperature-controlled chamber (ETAC, HISPEC HT210). A thermometer (FLUKE 179) was used for temperature monitoring with its sensor attached to the MEA during the measurement. An electronic load (Chroma 63103) was connected to the DMFC as an external load. It also functioned as performance recorder for current and voltage outputs. In active pump supplied DMFC hardware, the peristaltic pump (Longer, LEAD-1) was adopted for active fuel delivery. A piece of graphite block (POCO Graphite Inc., Decatur, TX) with a serpentine channel as the fuel flow field was attached to provide fuel distribution. The channel had a square cross-section with a depth and width of 0.75 mm. The length of a single parallel channel was 2.24 cm and the total flow length was 33.6 cm.

4. Prototype performance and discussion

4.1. Polarization characteristic

The passive prototype was loaded with 2 ml pure methanol and 5 ml DI water for polarization measurements. An activation process for the MEA was carried out by connecting it to an electronic load at a constant current mode (25 mA cm^{-2} at 25 °C, 35 mA cm^{-2} at 40 °C, and 45 mA cm^{-2} at 60 °C) for 5 min before the measurements. Polarization curves as well as power density curves were then measured and are given in Fig. 4(a) and (b) representing different operating temperatures, 25 °C, 40 °C and 60 °C, respectively. By eliminating the components between the pure methanol chamber and the water chamber in the passive prototype, the two chambers can be connected together for carrying diluted fuel. Accordingly, the prototype can be used as a conventional diluted fuel carrying DMFC for comparison measurements together with an active pump supplied DMFC. Since the required fuel concentration for most DMFC systems is in the range of 0.1–2.0 M, the diluted fuel carrying DMFC and the active pump supplied DMFC were fed by 1 M and 2 M diluted fuel, respectively, and hereafter [30]. For the active pump supplied one, the fuel flow rate was controlled at 2 ml min^{-1} by a peristaltic pump. Curves are shown in Fig. 4(a) and (b), in which, the active pump supplied DMFC exhibited a better performance than the diluted fuel carrying one, due to its high fuel concentration and enhanced fuel transportation by dynamic channel flow. However, the highest performance was achieved by passive prototype among these three DMFCs at all operating temperatures. Its maximum current densities were 32 mA cm^{-2} at 0.082 V under 25 °C, 43 mA cm^{-2} at 0.115 V under 40 °C, and 55 mA cm^{-2} at 0.140 V under 60 °C, while the peak power densities were 8.1 mW cm^{-2} at 0.349 V under 25 °C, 11.8 mW cm^{-2} at 0.376 V under 40 °C, and 16.8 mW cm^{-2} at 0.382 V under 60 °C, respectively, as labelled in Fig. 4(b). The passive methanol delivery driven by surface tension in the prototype was demonstrated by achieving an electrical output in this experiment. Meanwhile, the concentration and temperature sensitive surface tension driving effect are thought the reason for its relatively high performance. Under high current drain, the consumed methanol was able to be compensated for by the surface tension driving methanol delivery which also facilitated performance at increasing temperatures. Therefore, a higher fuel concentration can be achieved in the passive prototype, whereas the fuel concentration in the other DMFCs were fixed and slightly decreased due to methanol consumption during the operation.

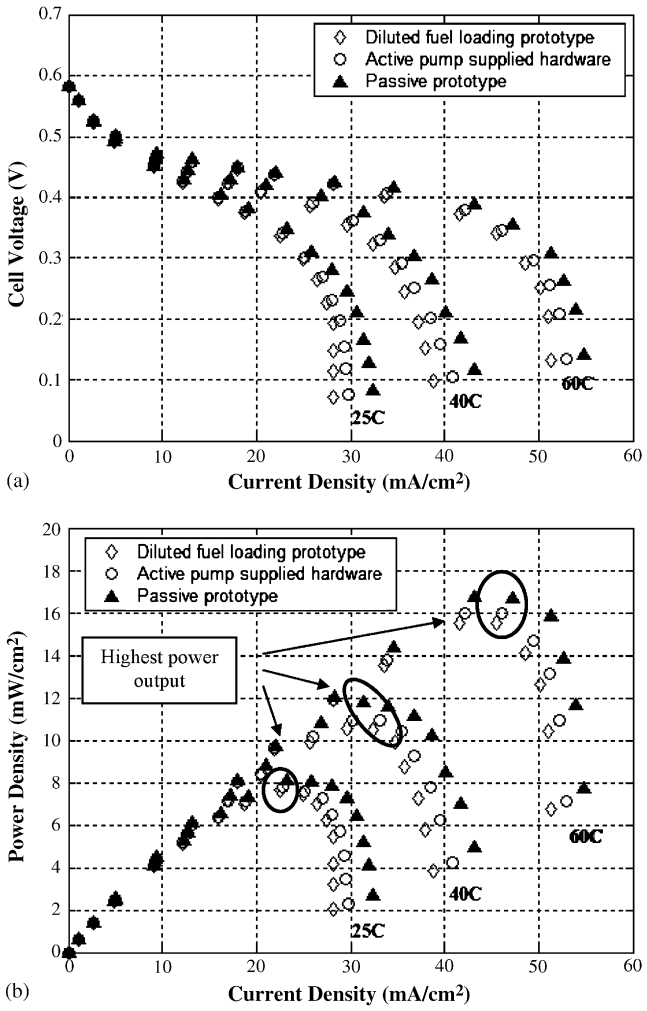

Fig. 4. (a) Polarization and (b) power density curves for three types of DMFCs operated at 25 °C, 40 °C, and 60 °C, 1 M methanol for the diluted fuel loading prototype, 2 M methanol at 2 ml min^{-1} for the active pump supplied hardware, and 2 ml pure methanol, 5 ml DI water for the passive prototype. The highest power output points of the active pump supplied hardware and passive prototype at different operating times are labeled.

4.2. Operating time

Subsequently, a demonstration experiment for continuity of surface tension driving methanol delivery in the passive prototype and its operating time was carried out. The same fuel loading amount, 2 ml pure methanol and 5 ml DI water, was applied as in the previous experiment. The electronic load set at constant resistance mode of 1 Ω was connected to the prototype for the power drain. The temperature of the environment was controlled and monitored at 25 °C. In the first 15 min of operation, the output voltage of the prototype rose from 0.128 V to 0.151 V and stayed stable at 0.166 V with current output of 160 mA after 30 min. To record the operating time of prototype, its voltage was monitored and recorded till the value fell down to 0.02 V, as given in Fig. 5. Operating time of more than 45 h was obtained by a passive prototype with 2 ml pure methanol. According to the output performance, the ability for continuous methanol delivery driven by surface tension in prototype was

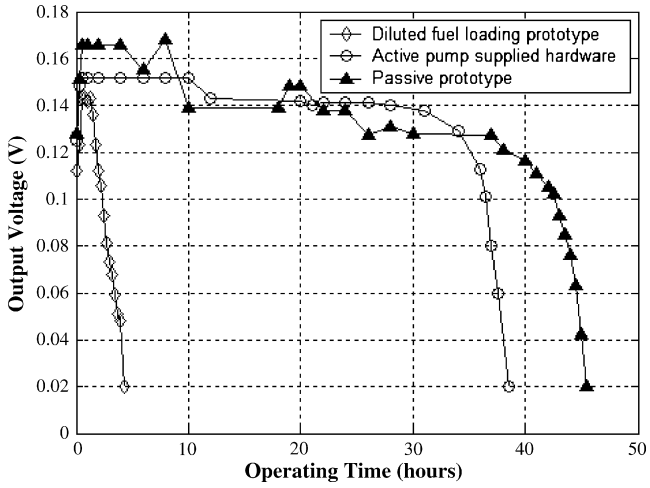

Fig. 5. Operating time of three types of DMFCs on constant 1 Ω load at 25 °C, 1 M methanol for diluted fuel loading prototype, 25 ml 2 M methanol at 2 ml min^{-1} for active pump supplied hardware, and 2 ml pure methanol for passive prototype.

demonstrated since no interruption happened during the electricity generation process. To compensate for water loss due to permeation and evaporation during its operation, an additional 12 ml DI water in total was refilled several times into the water chamber of the passive prototype.

As a comparison, the same experiment was executed on the diluted fuel carrying and active pump supplied DMFCs, respectively. The methanol delivery components were removed from the passive prototype and hence 7 ml of 1 M diluted methanol solution was filled in the prototype for the operation. The prototype lasted only around 5 h, which far less than with passive fuel delivery as can be seen in Fig. 5. With the same cell volume and fuel storage space, a more energetic content of methanol can be carried in the passive prototype and therefore contributes to its high cell power density as well as does the extended operating time. Even involving an additional volume for 12 ml DI water refilled in the passive prototype, its energy content (2 ml pure methanol) was still larger than that in 19 ml 1 M diluted fuel carrying DMFC (0.73 ml pure methanol). The peristaltic pump supplied DMFC was operated and compared to the passive prototype with the same amount of pure methanol. Accordingly, 25 ml of 2 M diluted methanol solution was fed to the DMFC hardware circularly at a flow rate of 2 ml min^{-1}. In Fig. 5, it's the operating time was found to be slightly less than that of the passive prototype with an equivalent 2 ml pure methanol. However, the voltage output was maintained more stable in comparison to that of the passive prototype, which is believed to benefit from steady fuel transportation in the anode channel. On the contrary, the methanol delivery in the passive prototype relies on an unstable capillary flow in the Teflon PTFE membrane, which was readily influenced by the internal environment of the water chamber especially by the accumulation of CO_2 bubbles from the anode reaction. In the first few hours of passive prototype operation, the methanol transportation was relatively drastic while not degraded by moderate CO_2 accumulation. Efficient methanol supply was able to be maintained. Consequently,

Table 1
Comparison between calculated and measured operating time of three types of DMFCs

DMFCs	Methanol amount (ml)	Fuel energy content (kJ)	Energy conversion yield (%) [31]	Power drawn from load (mW)	Calculated operating time (h)	Measured operating time (h)
Diluted fuel loaded	0.27	4.905	20	21.9	12.4	4.5
Passive prototype	2	36.330	27.2	74.2	45.2	
Active hardware	2	36.330	23.7	85.2	38.3	

a higher fuel concentration could be achieved and hence result in a better output performance at this early stage. As CO_2 bubbles were accumulated, they are released from a small hole on the side of water chamber, which is random and inefficient. As a result, the capillary pressure driven methanol flow will be influenced and therefore lead to a fluctuating performance during operation. Such a problem is neglectable in the active pump supplied DMFC, as its dynamic fuel flow provides efficient CO_2 removal from the reaction area. Therefore, a comparatively stable voltage output is able to be achieved by the active DMFC. However, the different operating time between them indicates that the efficiency of these two types of DMFCs is distinguished even though the same energy content was carried.

4.3. Fuel efficiency

Theoretically, the molar enthalpy of methanol combustion is 726.6 kJ mol^{-1} under standard conditions (298 K, 1 atm) [3]. Assuming the conversion yield is 20% at 25 °C, the energy released by the three different DMFCs from the electrochemical reaction is predictable and is given in Table 1 [31]. The power draw by a 1 Ω load in the above experiment can be found from the power density curves at 25 °C. Subsequently, the theoretical operating time for each DMFC is able to be calculated. In Table 1, the notable difference between the calculated and measured operating times is described which reveals the efficiency is overrated in the calculation. Therefore, an investigation of fuel efficiency becomes necessary to understand the operation. The comparative experiment is executed only between a passive prototype and active DMFC hardware as the diluted fuel carrying one is uncompetitive for long-duration operation.

To investigate the fuel utilization, the Faraday efficiency (η_F) is adopted for different operating temperatures. It is the ratio between theoretical volume of methanol needed by the load and to the experimentally determined consumption of methanol, as in Eq. (7), which tells how much of methanol is being used for the intended electrical energy production [16]:

$$\eta_F = \frac{\mathrm{Vol}_{\mathrm{MeOH}}^{\mathrm{Theoretical}}}{\mathrm{Vol}_{\mathrm{MeOH}}^{\mathrm{Experimental}}} = \frac{\int I(t)\,\mathrm{d}t \times \mathrm{Vol}_M}{x \times Fv} \tag{7}$$

where $I(t)$ is the current, Vol_M the molar volume of methanol (40 ml mol^{-1}), x the electrochemical valence of ions being transported through the DMFC, F the Faraday's constant (96,485 C mol^{-1}) and v is the volume of experiment consumed methanol.

In addition to the Faraday efficiency, the energy efficiency (η_E) is used for the cell efficiency investigation and is shown in Eq. (8) to reveal the percentage of energy from combination of methanol and oxygen resulting for the intended electrical energy [16]:

$$\eta_E = \frac{\mathrm{Energy}_{\mathrm{MeOH}}^{\mathrm{Electrical}}}{\mathrm{Energy}_{\mathrm{MeOH}}^{\mathrm{Content}}} = \frac{\int V(t) \times I(t)\,\mathrm{d}t}{6FEv/\mathrm{Vol}_M} \tag{8}$$

where $V(t)$ is the output voltage and E is the theoretical voltage ($E = 1.21$ at 25 °C).

The operating time measurements were executed at the highest power output points, as labelled in Fig. 4(b), for both types of DMFC at 25 °C, 40 °C and 60 °C, respectively. Two millilitres of pure methanol was used for each operation (25 ml 2 M fuel circularly fed at 2 ml min^{-1} for active pump supplied DMFC). In Fig. 6, their output voltages were recorded versus the operating time to 0.08 V for each temperature. The same trend in output performance as previous experiment was found for operation under 25 °C and 40 °C. Both DMFCs exhibited comparable operating times while that the passive prototype extended a few hours longer. However, its output voltage fluctuated during the operation compared to the stable performance of the active pump supplied one. Once the temperature rose to 60 °C, the output voltage of the passive prototype dropped very quickly in contrast to the active DMFC. Upon integrating the operating time according to above efficiency definitions, the corresponding efficiency can be calculated and is summarised in Table 2. The passive prototype exhibited a better Faraday efficiency and energy efficiency at moderate temperatures (25 °C and 40 °C). However, the superiority became smaller when the temperature

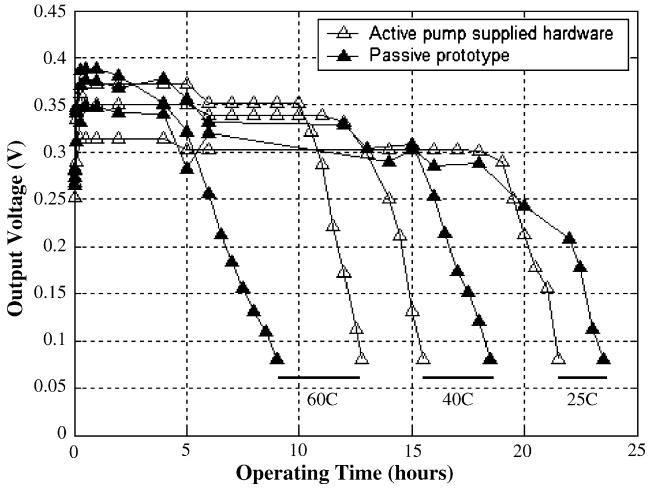

Fig. 6. Operating time comparison between the active pump supplied hardware and the passive prototype, at 25 °C, 40 °C and 60 °C. Twenty five millilitres of 2 M methanol at 2 ml min^{-1} for active pump supplied hardware, 2 ml pure methanol for passive prototype, operating at their highest power output points as labelled in Fig. 5.

Table 2
Fuel efficiency comparison of three types of DMFCs on constant load operation

DMFCs	25 °C	40 °C	60 °C
Passive prototype	$\eta_E = 6.92\%$ $\eta_F = 28.15\%$	$\eta_E = 8.18\%$ $\eta_F = 30.14\%$	$\eta_E = 4.81\%$ $\eta_F = 17.97\%$
Active hardware (without pump)	$\eta_E = 6.39\%$ $\eta_F = 26.01\%$	$\eta_E = 8.23\%$ $\eta_F = 30.04\%$	$\eta_E = 10.16\%$ $\eta_F = 35.37\%$
Active hardware (with pump)	$\eta_E = 3.47\%$ $\eta_F = 14.36\%$	$\eta_E = 6.14\%$ $\eta_F = 22.71\%$	$\eta_F = 8.46\%$ $\eta_F = 29.59\%$

rose. At 60 °C, a distinct operating time reduction of the passive prototype resulted in a steep fuel efficiency degradation. The phenomenon is believed to be due to competition between reaction kinetics and surface tension driving methanol delivery through capillaries in the separating membrane. High operating temperature enhances the electrochemical reaction kinetics, whereas it also facilitates the capillary methanol supply readily. Beyond the reaction consumption will present a high fuel concentration to the anode and hence lead to methanol crossover, which will reduce fuel efficiency slightly. Therefore, a gentle promotion in efficiency of the passive prototype from 25 °C to 40 °C (η_E: from 6.92% to 8.18%; η_F: from 28.15% to 30.14%) can be seen in Table 2 in comparing to active DMFC (η_E: from 6.39% to 8.23%; η_F: from 26.01% to 30.04%). The situation became worse at 60 °C since the volatilization loss of methanol and CO_2 release dominated other factors to exhaust methanol rapidly. On the contrary, the fuel loss from volatilization is tempered in the active DMFC due to its sealed fuel flow through a transportation pipe. Consequently, its efficiency is promoted by operating temperature.

The comparison of experimental measurements did not include the power consumption of the active pump. For micro scale applications, the active pump is normally integrated with the DMFC for fuel delivery and consumes part of the energy from its output. By neglecting the elevation loss and velocity difference along the flow length, the energy required by an active pump is used to compensate for the friction loss in the channel to maintain steady flow. The amount of this frictional energy loss per unit mass can be derived from Bernoulli's law and is described by the Fanning equation as given in Eq. (9):

$$h_f = \frac{\Delta P_f}{\rho} = \frac{C}{Re}\frac{L}{D_H}\frac{u^2}{2} \tag{9}$$

where ΔP_f is the frictional pressure drop, ρ the liquid density, Re the Reynolds number, C the friction factor which is 57 for square channel in our experiment [32], L the total length the liquid moves through, D_H the hydraulic diameter of the channel and u is the flow velocity.

Accordingly, the energy loss in flow channel will be 306.7 J, 220 J, and 178.3 J for 25 °C, 40 °C and 60 °C, respectively. As a piezoelectric pump is the most commonly used actuator in microfluidic applications and its efficiency can reach as high as 30%, the energy draw from the DMFC output to drive a micro pump will be 1022.3 J, 733.3 J, and 594.3 J for 25 °C, 40 °C and 60 °C. By involving such energy demand into active DMFC system, its efficiency degrades dramatically as shown in Table 2. Compared to a pump integrated active DMFC, the superiority of the passive prototype in efficiency improvement and cell volume savings becomes more competitive under moderate operating temperatures.

4.4. Load regulation

As a power supply, load regulation is another important criterion to evaluate the ability of a DMFC to remain within specified output limits for a predetermined load change. The load regulation is determined by Eq. (10) and it compares the change in output voltage at two loading extremes to the voltage produced at heavier loading:

$$\text{load regulation}\,(\%) = \frac{V_{Light} - V_{Heavy}}{V_{Heavy}} \times 100 \tag{10}$$

A small amount of load regulation thereby indicates a competitive ability of the DMFC to deliver a constant voltage to an external circuit load. Meanwhile, it also reduces the requirement on the auxiliary regulation circuit and hence simplifies the overall system, which has significant benefit for small-scale applications.

The comparative experiment on load regulation between the passive prototype and active DMFC was carried out at 25 °C and 40 °C since the volatilization loss of methanol in passive prototypes degrades the performance dramatically at 60 °C. Similarly, 2 ml pure methanol was loaded by the passive prototype and an equivalent 25 ml 2 M dilute fuel was fed circularly by a peristaltic pump to the active DMFC at a flow rate of 2 ml min^{-1}. The output performance of these two types of DMFC is shown in Fig. 7(a) and (b). For 25 °C, the load was working at a constant current mode of 23 mA cm^{-2} for 5 h, then was 15 mA cm^{-2} for 10 h and finally was 28 mA cm^{-2} till output voltage fell down to 0.1 V. The same time period was for operation at 40 °C, whereas the load was set at 33 mA cm^{-2}, 20 mA cm^{-2} and 38 mA cm^{-2}, respectively. The load regulation was calculated between operations with a light load (15 mA cm^{-2} for 25 °C, 20 mA cm^{-2} for 40 °C) and a heavy load (28 mA cm^{-2} for 25 °C, 38 mA cm^{-2} for 40 °C). In Fig. 7(a), the output voltage change of passive prototype is 0.141 V at 25 °C. Comparing the output voltage of 0.271 V on the heavy load, the load regulation was 52.03%. The operation at 40 °C achieved an output voltage change of 0.152 V and a load regulation of 55.88% compared to a heavy load voltage of 0.272 V, as can be seen in Fig. 7(b). Correspond-

Table 3
Fuel efficiency of three types of DMFCs on varying load operation

DMFCs	Energy in 2 ml methanol (J)	25 °C		40 °C	
		Output energy (J)	Efficiency (%)	Output energy (J)	Efficiency (%)
Passive prototype	35,024	2805.4	$\eta_E = 8.01$ $\eta_F = 29.54$	3372.4	$\eta_E = 9.63$ $\eta_F = 33.34$
Active hardware (without pump)		2312	$\eta_E = 6.60$ $\eta_F = 25.62$	2863.3	$\eta_E = 8.18$ $\eta_F = 29.83$
Active hardware (with pump)		1289.7	$\eta_E = 3.68$ $\eta_F = 11.95$	2130	$\eta_E = 6.08$ $\eta_F = 19.06$

ingly, the load regulation of the active DMFC was 71.74% for 25 °C and 88.32% for 40 °C. Therefore, the passive prototype exhibited better capability in its load regulation performance and hence represents a promising capability in practical applications.

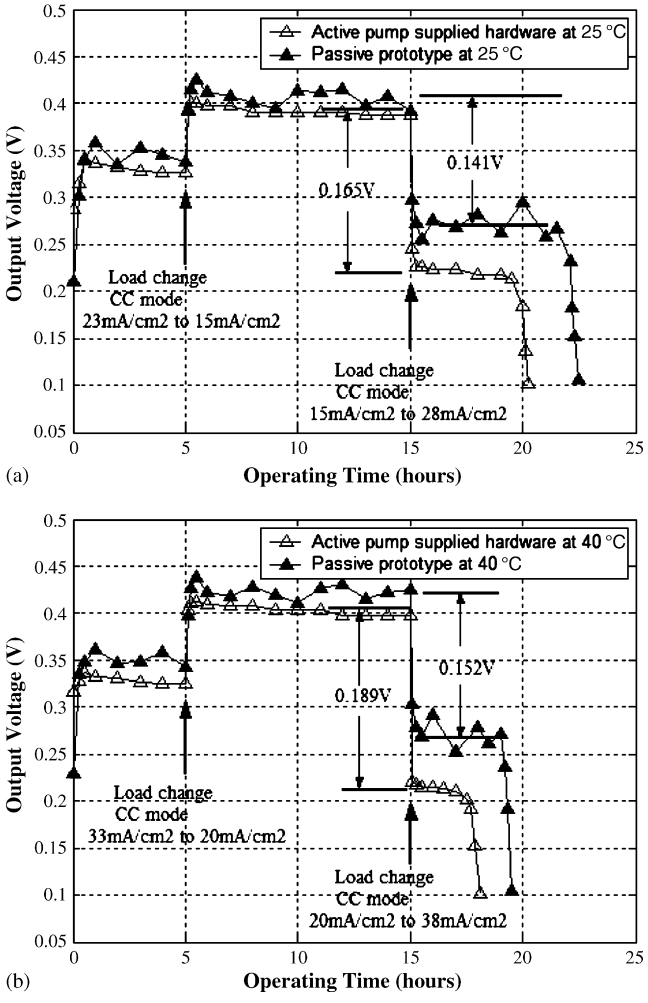

Fig. 7. Performance of two DMFCs on a varying load: 25 ml 2 M methanol at 2 ml min^{-1} for active pump supplied hardware and 2 ml pure methanol for passive prototype. (a) 25 °C, load change from 23 mA cm^{-2} to 15 mA cm^{-2} at 5 h and from 15 mA cm^{-2} to 28 mA cm^{-2} at 15 h on constant current mode, output voltage change 0.165 V for the active hardware and 0.141 V for the passive prototype; (b) 40 °C, load change from 33 mA cm^{-2} to 20 mA cm^{-2} at 5 h and from 20 mA cm^{-2} to 38 mA cm^{-2} at 15 h on constant current mode, output voltage change 0.189 V for active hardware and 0.152 V for the passive prototype.

Meanwhile, the efficiency of these two DMFCs on varying the load was also calculated and is given in Table 3. For the passive prototype, the efficiency had a notable improvement in both Faraday efficiency and energy efficiency (25 °C: $\eta_E = 8.01\%$, $\eta_F = 29.54\%$; 40 °C: $\eta_E = 9.63\%$, $\eta_F = 33.34\%$) for the two operating temperatures compared to previous operation on a constant load. However, there is no visible promotion in of the active DMFC and it was even getting worse from the energy consumption of the integrated pump, as shown in Table 3. The surface tension driving methanol delivery, which compensates the lack of methanol in responding to its consumption spontaneously under varied loading operations, is believed to be the major reason to for such high efficiency and small load regulation in the passive prototype.

5. Conclusion

A passive fuel delivery system operating with a surface tension driving effect has been proposed and demonstrated in this paper with a laboratory-made DMFC prototype. According to their difference in wettabilities, the spontaneous methanol and water flows exhibited an opposite motion in a single hydrophobic capillary. By separating these two liquids with a capillary containing a microfibrous Teflon PTFE membrane, a unidirectional methanol to water flow and therefore a passive fuel delivery and mixing effect were achieved in the DMFC prototype. With this approach, the passive prototype was able to operate with pure methanol, which significantly improved its power density compared to the conventional passive DMFC carrying a diluted methanol solution in the same fuel storage volume. Due to its consumption depending on the surface tension driving methanol supply, the polarization performance of this passive prototype is found to be better than the conventional passive and active DMFCs, which operate under fixed fuel concentrations. This approach of supplying methanol in a passive prototype also helped achieve a remarkable promotion in fuel utilization and efficiency compared to the active pump supplied DMFC, especially when they are operated by variable loading. Meanwhile, the passive prototype exhibited a better load regulation performance in contrast to the active DMFC. By saving extra power consumption on fuel supply actuators, the superiority of this passive DMFC prototype in its efficiency and system simplicity, is attractive for future applications in small-scale electronics.

References

[1] W. Vielstich, H. Gasteiger, A. Lamm, Handbook of Fuel Cell: Fundamentals, Technology, Applications, vol. 3, John Wiley & Sons, New York, 2003, pp. 337–339.
[2] W. Vielstich, H. Gasteiger, A. Lamm, Handbook of Fuel Cell: Fundamentals, Technology, Applications, vol. 1, John Wiley & Sons, New York, 2003, pp. 305–322.
[3] J. Larminie, A. Dicks, Fuel Cell System Explained, 2nd ed., John Wiley & Sons, New York, 2003, pp. 1–5.
[4] B. Cook, An Introduction to Fuel Cells and Hydrogen Technology, Canada Heliocentris, Vancouver, BC, 2002, V6R-1S2, pp. 1–8.
[5] Kordesch, Karl, G. Simader, Fuel Cells and Their Applications., VCH, New York, 1996, pp. 1–9.
[6] H. Dohle, J. Divisek, J. Mergel, H.F. Oetjen, C. Zingler, D. Stolten, Proceedings of the Fuel Cell Seminar, 30 October–2 November, Portland, OR, USA, 2000, p. 16.
[7] C. He, H.R. Kunz, J.M. Fenton, J. Electrochem. Soc. 144 (1997) 970–979.
[8] S. Park, Y.Y. Tong, A. Wieckowski, M.J. Weaver, Langmuir 18 (2002) 3233–3240.
[9] X. Ren, T.A. Zawodzinski Jr., F. Uribe, H. Dai, S. Gottesfeld, in: S. Gottesfeld, G. Halpert, A. Landgrebe (Eds.), The Electrochemical Society Proceedings Series, Pennington, NJ, 1995, p. 284 (PV 95-23).
[10] Y.J. Kim, W.C. Choi, S.I. Woo, W.H. Hong, J. Membr. Sci. 238 (2004) 213–222.
[11] H. Uchida, Y. Mizuno, M. Watanabe, J. Electrochem. Soc. 149 (2002) A682–A689.
[12] Y.C. Si, J.C. Lin, H.R. Kunz, J.M. Fenton, J. Electrochem. Soc. 151 (2004) A463–A469.
[13] T. Zhang, Q.M. Wang, J. Power Sources 158 (2006) 169–176.
[14] D. Kim, E.A. Cho, S.A. Hong, I.H. Oh, H.Y. Ha, J. Power Sources 130 (2004) 172–177.
[15] R. Chen, T.S. Zhao, J.G. Liu, J. Power Sources 157 (2006) 351–357.
[16] J.G. Liu, T.S. Zhao, R. Chen, C.W. Wong, Electrochem. Commun. 7 (2005) 288–294.
[17] T. Shimizu, T. Momma, M. Mohamedi, T. Osaka, S. Sarangapani, J. Power Sources 137 (2004) 277–283.
[18] R. Luharuka, C.F. Wu, P.J. Hesketh, Sens. Actuators A 112 (2004) 187–195.
[19] S.C. Yao, X. Tang, C.C. Hsieh, Y. Alyousef, M. Vladimer, G.K. Fedder, C.H. Amon, Energy 31 (2006) 636–649.
[20] J. Lee, C.J. Kim, J. Microelectromech. Syst. 9 (2000) 171–180.
[21] A. Frohn, N. Roth, Dynamics of Droplets, Springer-Verlag, New York, 2000, pp. 1–8.
[22] Burdon, R. Stanley, Surface Tension and the Spreading of Liquids, 2nd ed., Cambridge University Press, 1949, p. 72.
[23] B.R. Munson, D.F. Young, T.H. Okiishi, Fundamentals of Fluid Mechanics, Wiley, New York, 2002, pp. 26–28.
[24] R.M. Felder, R.W. Rousseau, Elementary Principles of Chemical Processes, John Wiley, New York, 2000, p. 313.
[25] J. Zahka, Millipore Microelectronics Applications Note MA 101, 14 September, 1998.
[26] S. Middleman, An Introduction to Fluid Dynamics: Principles of Analysis and Design, John Wiley & Sons, New York, 1998, p. 40.
[27] D.S. Kim, K.C. Lee, T.H. Kwon, S.S. Lee, J. Micromech. Microeng. 12 (2002) 236–246.
[28] Y. Feng, Z. Zhou, X. Ye, J. Xiong, Sens. Actuators A 108 (2003) 138–143.
[29] B. K, I. Oh, S. Hong, H.Y. Ha, Electrochim. Acta 50 (2004) 781–785.
[30] J.H. Shim, I.G. Koo, W.M. Lee, Electrochim. Acta 50 (2005) 2385–2391.
[31] G. Apanel, E. Johnson, Fuel Cell Bulletin, 2004 11 (2006) 12–17.
[32] H. Lamb, Hydrodynamics, 6th ed., Cambridge Univ. Press, Cambridge, 1945, pp. 20–25.